

Efficient Quantum-Dot Light-Emitting Diodes Enabled via a Charge Manipulating Structure

Rongmei Yu, Furong Yin, Dawei Zhou, Hongbo Zhu,* and Wenyu Ji*



Cite This: *J. Phys. Chem. Lett.* 2023, 14, 4548–4553



Read Online

ACCESS |



Metrics & More

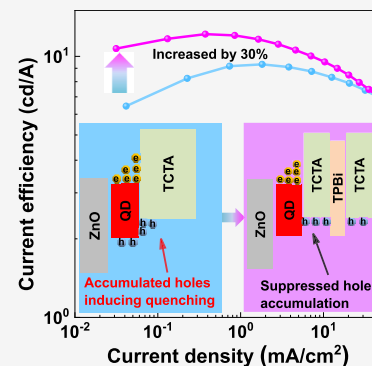


Article Recommendations



Supporting Information

ABSTRACT: Charge carriers are the basic physical element in an electrically driven quantum-dot light-emitting diode (QLED), which acts as a converter transforming electric energy to light energy. Therefore, it is widely sought after to manage the charge carriers for achieving efficient energy conversion; however, to date, there has been a lack of understanding and efficient strategies. Here, an efficient QLED is achieved by manipulating the charge distribution and dynamics with an n-type 1,3,5-tris(*N*-phenylbenzimidazole-2-yl)benzene (TPBi) layer embedded into the hole-transport layer. Compared with the control QLED, the maximum current efficiency of the TPBi-containing device is enhanced over 30%, reaching 25.0 cd/A, corresponding to a 100% internal quantum efficiency considering the ~90% photoluminescence quantum yield of the QD film. Our results suggest that there is still a great deal of room to further improve the efficiency in a standard QLED by subtly manipulating the charge carriers.



Due to their unique photoelectrical properties, such as high color purity, near unity photoluminescence quantum yield, large absorption cross section, and quasi-discrete energy levels, colloidal quantum dots (QDs) are emerging as an attractive class of luminescent materials for light-emitting diodes (referred to as QLEDs), laser diodes, and down-conversion layers.^{1–11} In the last three decades, huge progress has been made regarding QLEDs as a potential alternative technology for display and lighting applications.^{12–14} Various QD designs, such as alloying shell, gradient energy level engineering, and selenium throughout the core/shell, are reported to improve the performance of QLEDs. Benefiting from the advance of QD synthesis, the maximum external quantum efficiency of the red, green, and blue three-primary-color QLEDs has been over 20%, the theoretical limit value for planar devices without any light outcoupling technology. However, besides the QDs themselves, there is still much room to improve device performance by controlling the charge dynamics with a deliberate device design.^{15–22}

In general, the charge dynamics in an electrically driven device refers to three processes, including charge injection, charge transport, and charge recombination,^{23–26} which can be separately optimized. The charge injection is dominantly related to the interfaces between electrodes and charge-injection layers. An ohmic contact is desired to provide efficient charge injection. The charge transport is usually evaluated by the mobility of electrons or holes in the charge transport layers and barriers between different functional layers, which also determines the charge distribution in the devices. It is noteworthy that density of states is also relatively crucial for charge conduction,²⁷ which was often overlooked previously. The charge recombination refers to energy

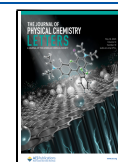
conversion of excited electrons through radiative and non-radiative channels, where photons are obtained by the radiative process. The nonradiative processes include the well-known Auger recombination and heating effect,^{28–31} which are usually aggravated by the charge accumulation caused by imbalanced charge injection or/and interface barriers.^{17,32} Moreover, charge accumulation can also lead to extra voltage/energy consumption, hence causing dramatic decrease of power efficiency of QLEDs especially under high driving voltages. Therefore, it is critical to manage the charge processes within the QLEDs from the luminous efficiency point of view.

Various approaches have been proposed to regulate the charge carriers, aiming to promote the device efficiency and operational lifetime.^{15–17,32} Dai et al. reported that the efficiency and operational lifetime of QLEDs could be improved by balancing the charge injection with a PMMA electron-blocking layer.³² Great improvement has also been demonstrated by inserting Al₂O₃ thin layers to inhibit the electron leakage.¹⁶ An alternative solution to inhibit the electron leakage has also been proposed by inserting phosphorescent molecules as the electron harvester, which then could be used to excite the QDs by virtue of the energy transfer.¹⁵ Ji et al. declared that the device efficiency can be markedly enhanced by inserting a 1,3,5-tris(*N*-phenylbenzimi-

Received: March 30, 2023

Accepted: May 5, 2023

Published: May 9, 2023



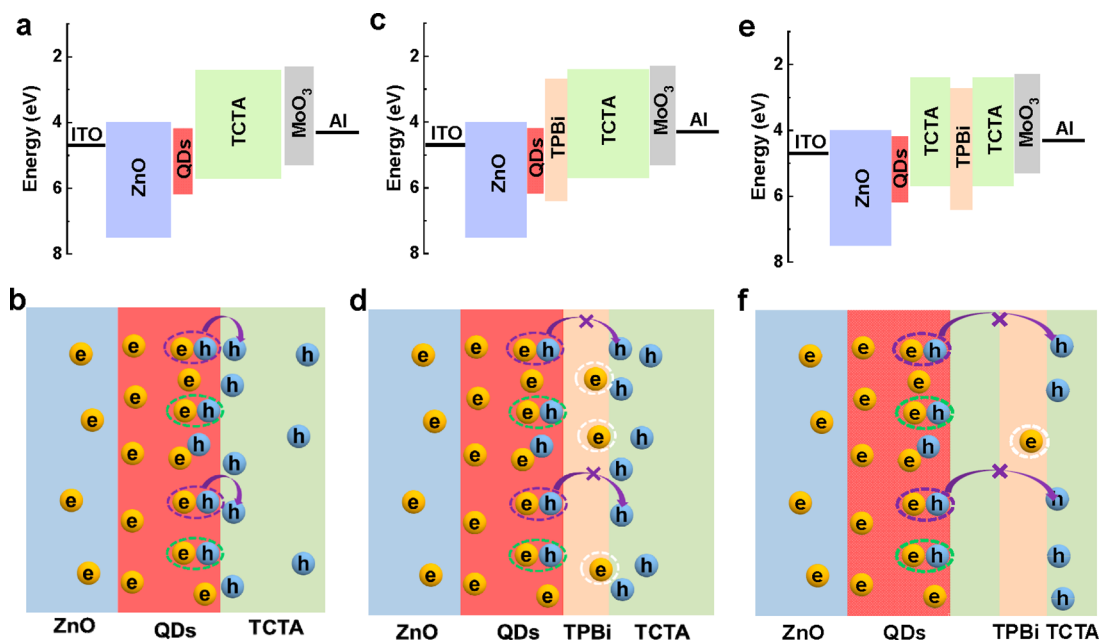


Figure 1. (a, c, and e) Diagrams of energy levels of the materials used in this work, (b, d, and f) Schematic illustration for the distribution and accumulation of the charges in different devices. All the energy levels are cited from refs 1 and 17. The TPBi layer moves the hole accumulation zone to the TPBi/TCTA interface. The electrons and holes in purple and green ellipses represent the excitons; the leaked electrons are marked with white ellipses. The purple arrows indicate the emission quenching of the excitons caused by the accumulated holes.

dazole-2-yl)benzene (TPBi) between QDs and hole-transporting layer (HTL), which suppressed the nonradiative recombination induced by the accumulated holes.¹⁷ Nevertheless, although the device efficiency can be dramatically improved by either balancing the charge injection estimated through the apparent current density of single-carrier devices or suppressing the quenching effect induced by the accumulated holes, the understanding for the charge effect is so far still empirical or hypothetical.

In this work, the hole distribution and electron leakage in the QLEDs are examined by transient electroluminescence (TrEL) measurements. The hole accumulation at QDs/HTL interface is highly suppressed by inserting a TPBi layer at QDs/HTL interface or in the middle of the HTL. Compared with the QLED where the TPBi layer is positioned at the QD/HTL interface (named i-TPBi), the electron leakage from the QDs is largely restrained by moving the TPBi layer into the HTL (referred to as h-TPBi). As a result, the current efficiency (CE) of h-TPBi-containing QLEDs is further enhanced by a factor of 15% compared to the optimal i-TPBi device, without sacrificing power efficiency (PE), which is instead also improved by 15%. Then the CE and PE of the h-TPBi device are respectively enhanced by 31% and 27% in comparison to those of QLEDs without a TPBi layer. These results indicate that the h-TPBi hole-modulating layer does not lead to extra voltage loss nor power consumption. This should be attributed to the synergetic effect originating from the suppression of hole accumulation and electron leakage.

The standard inverted structure of glass/ITO/ZnO (~40 nm)/QDs (~25 nm)/4,4',4''-Tris(*N*-carbazolyl)-triphenylamine (TCTA, ~50 nm)/MoO₃ (~8 nm)/Al (~100 nm) was employed to investigate the influence of charge distribution on the device performance, where ZnO, QDs, and TCTA were used as the ETL, emissive layer, and HTL, respectively. In order to modulate the hole distribution, a TPBi hole-blocking layer with different thicknesses was inserted at

the QDs/TCTA interface or in the middle of the TCTA HTL (with the structure of TCTA/TPBi/TCTA). Before fabrication, the ITO substrates were ultrasonically cleaned in acetone, ethanol, and deionized water in sequence for 15 min each and then dried by nitrogen flow. The detailed procedures for the device fabrication can be found in our previous reports.^{33–35} The CdSe/ZnS QDs were purchased from *Najing Technology Corp.*, and other materials were purchased from *Xi'an Polymer Light Technology Corp.* The optical properties of QDs were characterized in our previous work. All the devices were encapsulated with cover glasses and UV-curable epoxy resin.

The transient electroluminescence (TrEL) response was recorded through a home-built system consisting of a photomultiplier tube (Zolix PMTH-S1-CR131), a digital oscilloscope (RIGOL DS4054), and a signal generator (RIGOL DGS102). The driving pulse width was 400 μs with a repetition rate of 1 kHz and amplitude of 4 V. The current density–voltage–luminance (*J–V–L*) properties and electroluminescence (EL) spectra were obtained by a programmable Keithley 2400 power supply combined with a Minolta Luminance Meter and an Ocean Optics Maya 2000-PRO spectrometer. The impedance spectroscopy measurements were implemented through a precision LCR meter (Tonghui TH2829C) at a frequency of 500 Hz, and the oscillation amplitude of the AC voltage was 100 mV. All the measurements were performed at room temperature.

For a typical QLED, the energy level diagram can be commonly depicted as shown in Figure 1a. The large hole injection barrier between QDs and TCTA HTL leads to serious accumulation of holes, which is detrimental to the device performance, including efficiency and operational lifetime. It has been reported that the accumulated holes at the QDs/HTL interface can quench the QD emission, as illustrated in Figure 1b.¹⁷ To avoid the quenching effect induced by the accumulated holes, a feasible approach is to

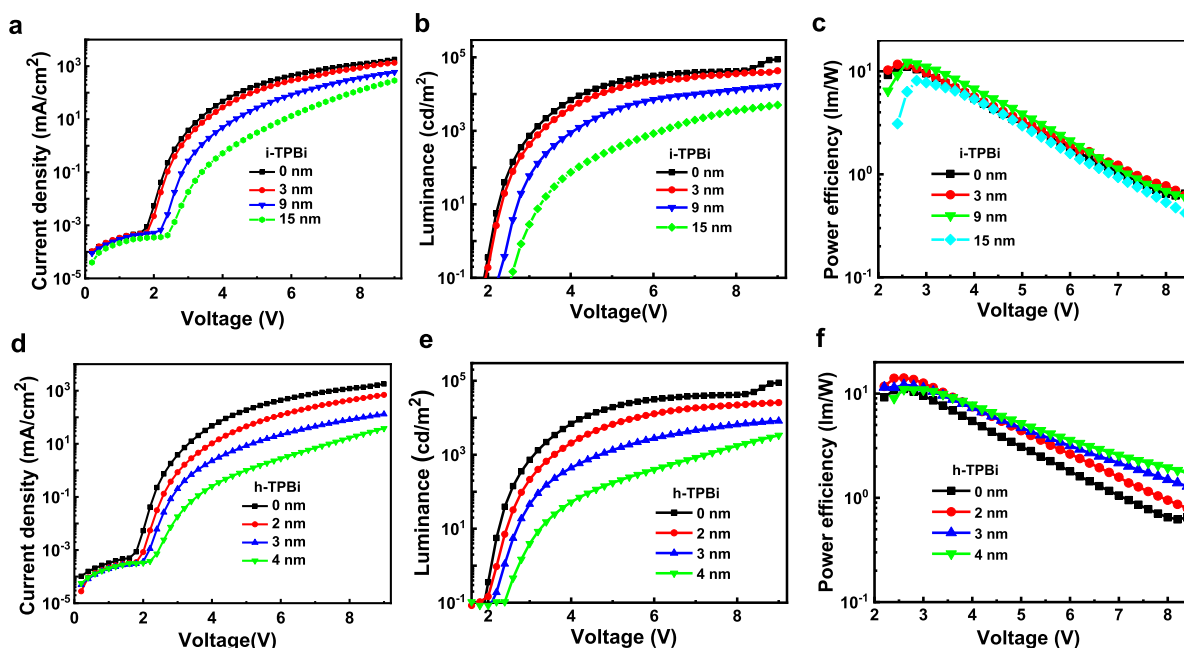


Figure 2. (a and d) Current density (J), (b and e) luminance (L), and (c and f) power efficiency (PE) properties of the QLEDs as the function of applying voltages. The top panel is the devices with TPBi (i-TPBi) at QDs/TCTA interface, and the bottom one is the case where the TPBi (h-TPBi) is positioned at the middle of TCTA HTL. The QLED with 0 nm TPBi is used as the control device.

insert a TPBi (referred to as i-TPBi) spacer between QDs and HTL as depicted in Figure 1c. Due to the hole-blocking effect of the i-TPBi layer, the hole accumulation zone is moved to the TPBi/TCTA interface (Figure 1d). Hence, the quenching effect can be highly suppressed in the i-TPBi-containing device. As observed in Figure 2a, the current densities of the QLEDs decrease gradually as the i-TPBi thickness increases, which is attributed to the hole-blocking effect of n-type TPBi small molecules. Correspondingly, the device luminance is also reduced owing to the reduced hole injection and hence low density of charge carriers. Moreover, the turn-on voltage (defined as the voltage for the device at luminance of 0.1 cd/m^2) is increased from 2.0 to 2.4 V. However, compared with the control device without i-TPBi, the peak efficiencies of the QLEDs are enhanced as observed from Figures 2c and S1. The device performance is also summarized in Table 1. The peak

Table 1. Summary of the Device Performance with i-TPBi Layers^a

i-TPBi	0 nm (control)	3 nm	9 nm	15 nm
L_{max} (cd/m^2)	92600	81300	22600	7180
CE_{max} (cd/A)	19.5	20.0	22.3	15.8
PE_{max} (lm/W)	23.3	24.6	25.8	17.0
V_{on} (V)	2.0	2.2	2.4	2.8
fwhm (nm)	34.7	34.7	32.9	39.6

^a L_{max} is the maximum luminance; CE_{max} and PE_{max} represent peak current efficiency and power efficiency, respectively; V_{on} is the driving voltage for the device at luminance of 0.1 cd/m^2 .

current efficiency (CE) of the QLED with a 9 nm i-TPBi layer is increased to 22.3 cd/A , 14.4% higher than that (19.5 cd/A) of the control device. It is worth noting that the enhancement for the peak power efficiency (PE) is 10.7%, lower than that of CE. This result indicates that although the device efficiency is improved due to the hole blocking of TPBi, extra power or voltage loss occurs due to hole accumulation. Furthermore, all

the QLEDs enjoy a similar PE trend with voltage increase as shown in Figure 2c, revealing that the hole accumulation is not reduced but only changes its position.

The EL spectra of the QLEDs are shown in Figure S2. We can see that a discernible contribution from TPBi emission in the short wavelength region emerges for the device with a 15 nm TPBi layer. This reveals that the electrons in the QDs could be leaked into the TPBi layer, where excitons are formed. Thereby, the device performance is greatly reduced. A feasible method to solve the above issues is described in Figure 1e,f, where a TPBi layer (named h-TPBi) is deposited in the middle of the TCTA HTL. This h-TPBi layer plays a dual role in modulation of the hole distribution, slowing the hole transport in the TCTA HTL and keeping the hole accumulation (if any) away from QDs. As shown in Figure 2d–f and Table 2, the h-TPBi-containing QLEDs present a

Table 2. Summary of the Device Performance with h-TPBi Layers

h-TPBi	0 nm (control)	2 nm	3 nm	4 nm
L_{max} (cd/m^2)	92600	25650	8190	3356
CE_{max} (cd/A)	19.5	25.6	22.7	22.5
PE_{max} (lm/W)	23.3	29.6	25.4	23.1
V_{on} (V)	2.0	2.2	2.4	2.6
fwhm (nm)	34.7	33.7	32.9	33.3

similar trend as that of i-TPBi based devices; that is, both the current density and luminance are reduced with increasing h-TPBi thicknesses and device efficiencies are largely enhanced. The optimal device with a 2 nm h-TPBi (thinner than the optimal i-TPBi of 9 nm) possesses peak CE (PE) of 25.6 cd/A (29.6 lm/W), increased by 31% (27%) compared with that of the control device. These results demonstrate that the QLEDs with h-TPBi are more efficient than the i-TPBi case. The reason will be explored by TrEL measurements.

Figure 3a shows the falling edges of the QLEDs with different i-TPBi thicknesses driven under a 4 V voltage pulse

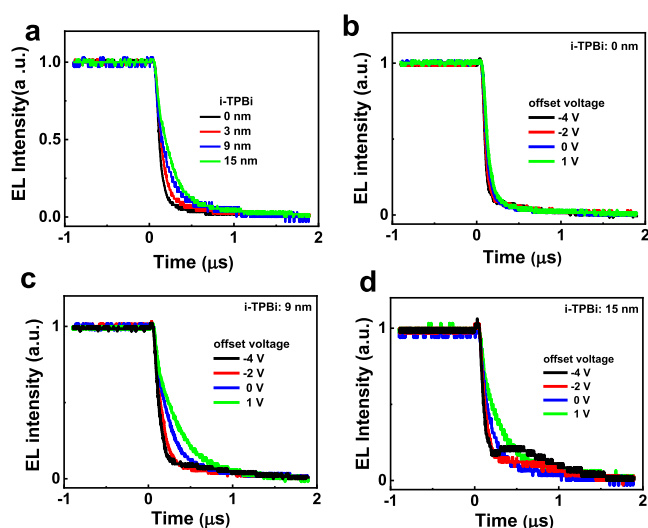


Figure 3. (a) Falling edges of the TrEL spectra for the devices containing i-TPBi layers with different thicknesses, without offset voltage. Offset voltage-dependent falling edges for (b) control, (c) 9 nm i-TPBi, and (d) 15 nm i-TPBi layers.

(the whole TrEL response can be found in Figure S3a). We can see that the falling edges are prolonged with increasing i-TPBi thicknesses. This means that there is a slow back transfer process for the charges, which provide additional charges to the QDs for the formation of excitons and then a slow EL decay in thicker i-TPBi devices. Given the very low hole mobility in QD films,²⁶ we deduce that the slow back-transfer charge species are the electrons leaked into the i-TPBi layers. As depicted in Figure 1d, the electrons leaked into the i-TPBi layer could be transferred back to the QDs after turning off the driving voltage, thereby providing an additional exciton-formation channel for the QDs and prolonging EL decay. In order to further confirm the above hypothesis, the offset-voltage-dependent EL decay is probed as shown in Figure 3b–d because the dynamics of the accumulated charges are sensitive to the electrical field.³⁶ The control device without a TPBi layer exhibits nearly the same EL decays at different offset voltages as shown in Figure 3b, which is attributed to the single-source accumulated charges. Specifically, in the control QLED, the charges are dominantly accumulated at the QDs/TCTA interface, which can inject into the QDs immediately and form excitons once the driving voltage is turned off. Thus, the offset voltage can hardly affect the back transfer process of the charges (i.e., electrons as discussed above). In stark contrast, the back transfer process of the leaked electrons at the i-TPBi/TCTA interface is accelerated under negative offset voltage and slowed under positive offset voltage. As shown in Figure 3c, the falling edges of TrEL response for the device with 9 nm i-TPBi verify dependence of leaked electrons on the offset voltages. This EL decay becomes more sensitive to the offset voltage for the device with a thicker i-TPBi layer. As can be seen from Figure 3d, an overshoot even occurs for the QLED with 15 nm i-TPBi layer under a -4 V offset voltage. This provides substantial evidence that the electrons are indeed leaked into the i-TPBi layer. From the device efficiency point of view, the optimal thickness of the i-TPBi layer is 9 nm. It is noteworthy that hole accumulation at the i-TPBi/TCTA

interface is inevitable due to the thicker i-TPBi layer. Then, the extra power or voltage loss mentioned above occurs owing to the dual effect of hole accumulation and electron leakage.

The TrEL responses of the h-TPBi devices are also investigated to evaluate the charge distribution in the QLEDs. The EL decay is prolonged with increasing thickness of h-TPBi up to 3 nm as shown in Figures 4a and S3b.

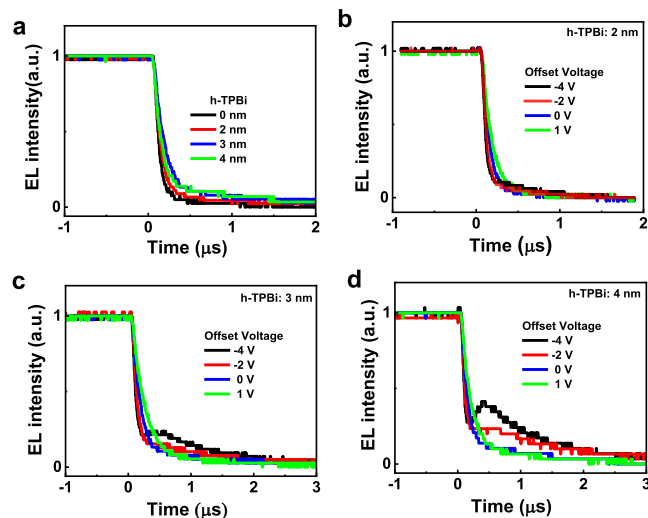


Figure 4. (a) Falling edges of the TrEL spectra for the devices containing h-TPBi layers with different thicknesses, without offset voltage. Offset voltage-dependent falling edges for devices with (b) 2 nm, (c) 3 nm, and (d) 4 nm i-TPBi layers.

However, a thicker h-TPBi layer (4 nm) leads to an accelerated EL decay. Compared with the i-TPBi QLEDs, the h-TPBi devices displays a similar but quite weak dependence of EL decay on the offset voltage (Figure 4b). Even so, a stronger overshoot can be observed for the devices with thicker h-TPBi layers driven under negative offset voltage as depicted in Figure 4c,d, which implies that the electrons are indeed leaked into the h-TPBi layer. It is worth pointing out that the weak dependence of falling edge on the offset voltage for the device with an optimal h-TPBi layer (2 nm) should stem from reduced charge accumulation. To verify this, the capacitance properties of these QLEDs are measured and the results are shown in Figure 5. In general, the negative capacitance at high driving voltage is attributed to the inductive effect induced by the accumulated charges. For both the control and i-TPBi based QLEDs, the device capacitance becomes negative under high driving voltages as shown in Figure 5a, which is the indicator of charge accumulation inside the devices. In sharp contrast, the h-TPBi based devices always possess positive

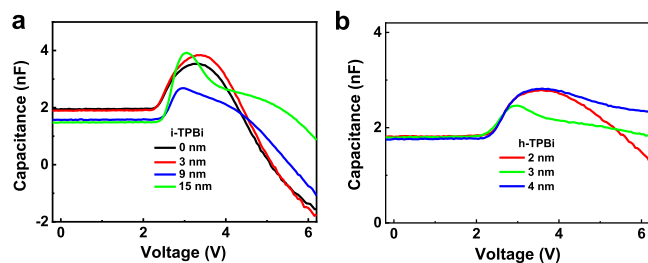


Figure 5. Capacitance versus voltage curves for (a) i-TPBi and (b) h-TPBi based QLEDs.

capacitance in the whole operating voltage region (Figure 5b). These results demonstrate that there is little charge accumulation in the h-TPBi devices, which might be the origin of higher PE under high driving voltages for the h-TPBi device as shown in Figure 2f. Then, we can reach the conclusion that, for the QLEDs, a thin h-TPBi layer is more efficient than the case of i-TPBi. Moreover, the main role of the h-TPBi is to reduce or slow the hole injection but not change the position of the hole accumulation.

The influence of TPBi layers on the EL turn-on behavior is also evaluated by recording the rising edges of the TrEL response, and the results are plotted in Figure S4. It can be seen that, similar to the falling edges shown in Figures 3 and 4, the rising edges are also sensitive to the V_{os} . A negative V_{os} leads to delayed and slow EL turn-on, which should be due to the different charging time for the devices. Negative offset voltages induce a reverse charging of the devices. Hence, the charging time is prolonged when a positive driving voltage is applied to the QLEDs. Additionally, enhanced overshoot of the TrEL for the devices with thicker TPBi layers is found as shown in Figures S4a and 4c when a negative V_{os} is applied to the devices. This is attributed to the different distribution of charges within the devices.

In summary, highly efficient usage of charges in the QLEDs is achieved by inserting a hole-modulating layer in the middle of the TCTA HTL. Then, the hole accumulation and electron leakage are optimized simultaneously, which avoids both exciton quenching and charge loss. As a result, both current efficiency and power efficiency are enhanced obviously. Especially, the h-TPBi devices possess higher power efficiency under high driving voltages owing to the elimination of the hole accumulation. Our results provide further insights into the charge modulation; that is, charge distribution, rather than the apparent charge balance, is the more fundamental parameter affecting the formation efficiency of excitons. Moreover, a more efficient device is achieved by reducing hole injection in an electron-dominating QLED, which further verifies that efficient and enough electron injection into the QDs is indispensable in present hybrid QLEDs.^{2,3} This unique working mechanism deserves further investigation to optimize device design.

■ ASSOCIATED CONTENT

SI Supporting Information

The Supporting Information is available free of charge at <https://pubs.acs.org/doi/10.1021/acs.jpcllett.3c00853>.

Current efficiency–current density curves of the QLEDs with and without TPBi layers, EL spectra (PDF)

Transparent Peer Review report available (PDF)

■ AUTHOR INFORMATION

Corresponding Authors

Hongbo Zhu – State Key Laboratory of Luminescence and Applications, Changchun Institute of Optics, Fine Mechanics and Physics, Chinese Academy of Sciences, Changchun 130033, China; Email: zhbcioimp@163.com

Wenyu Ji – College of Physics, Jilin University, Changchun 130023, China; orcid.org/0000-0003-2932-5119; Email: jiwy@jlu.edu.cn

Authors

Rongmei Yu – Henan International Joint Laboratory of MXene Materials Microstructure, College of Physics and Electronic Engineering, Nanyang Normal University, Nanyang 473061, China; orcid.org/0000-0001-8885-4518

Furong Yin – Henan International Joint Laboratory of MXene Materials Microstructure, College of Physics and Electronic Engineering, Nanyang Normal University, Nanyang 473061, China

Dawei Zhou – Henan International Joint Laboratory of MXene Materials Microstructure, College of Physics and Electronic Engineering, Nanyang Normal University, Nanyang 473061, China

Complete contact information is available at:

<https://pubs.acs.org/10.1021/acs.jpcllett.3c00853>

Author Contributions

W.J. and H.Z. proposed the idea and designed the experiments. R.Y. carried out the device fabrication and simulation. F.Y. and D.Z. performed the photoelectrical characterizations. All authors discussed the results and have given approval to the final version of the manuscript.

Notes

The authors declare no competing financial interest.

■ ACKNOWLEDGMENTS

This work was supported by the program of the National Natural Science Foundation of China (Nos. 12274173, 11974141, 12074148, and 62222410); the Key Science Fund of Educational Department of Henan Province of China (22A140008); Research Projects of Henan Science and Technology Committee (222102210235); and Open Project of Key Lab of Special Functional Materials of Ministry of Education, Henan University (KFKT-2022-XX).

■ REFERENCES

- Jang, E.; Jang, H. Reviews: Quantum Dot Light-Emitting Diodes. *Chem. Rev.* **2023**, *123* (8), 4663–4692.
- Liu, M.; Yazdani, N.; Yarema, M.; Jansen, M.; Wood, V.; Sargent, E. H. Colloidal Quantum Dot Electronics. *Nat. Electron.* **2021**, *4* (8), 548–558.
- Shu, Y.; Lin, X.; Qin, H.; Hu, Z.; Jin, Y.; Peng, X. Quantum Dots for Display Applications. *Angew. Chem. Int. Edit.* **2020**, *59* (50), 22312–22323.
- Kim, T.; Kim, K. H.; Kim, S.; Choi, S. M.; Jang, H.; Seo, H. K.; Lee, H.; Chung, D. Y.; Jang, E. Efficient and Stable Blue Quantum Dot Light-Emitting Diode. *Nature* **2020**, *586* (7829), 385–389.
- Xiang, H.; Wang, R.; Chen, J.; Li, F.; Zeng, H. Research Progress of Full Electroluminescent White Light-Emitting Diodes Based on a Single Emissive Layer. *Light Sci. Appl.* **2021**, *10*, 206.
- Lim, J.; Park, Y. S.; Klimov, V. I. Optical Gain in Colloidal Quantum Dots Achieved with Direct-Current Electrical Pumping. *Nat. Mater.* **2018**, *17* (1), 42–49.
- Park, Y.-S.; Roh, J.; Diroll, B. T.; Schaller, R. D.; Klimov, V. I. Colloidal Quantum Dot Lasers. *Nat. Rev. Mater.* **2021**, *6* (5), 382–401.
- Yu, P.; Cao, S.; Shan, Y. L.; Bi, Y. H.; Hu, Y. Q.; Zeng, R. S.; Zou, B. S.; Wang, Y. J.; Zhao, J. L. Highly Efficient Green InP-Based Quantum Dot Light-Emitting Diodes Regulated by Inner Alloyed Shell Component. *Light Sci. Appl.* **2022**, *11*, 162.
- Yu, H.; Zhang, J.; Long, T.; Xu, M.; Feng, H.; Zhang, L.; Liu, S.; Xie, W. Efficient All-Blade-Coated Quantum Dot Light-Emitting Diodes through Solvent Engineering. *J. Phys. Chem. Lett.* **2020**, *11* (21), 9019–9025.

- (10) Hong, Z.; Zou, Y.; Li, Y.; Cai, L.; Chen, Z.; Zang, J.; Bai, G.; Li, Y.; Chen, J.; Wu, Y.; Jiang, C.; Song, T.; Sun, B. In Situ Ligand-Exchange in Solid Quantum Dots Film Enables Stacked White Light-Emitting Diodes. *Adv. Opt. Mater.* **2022**, *10* (20), 2200918.
- (11) Kim, D. C.; Yun, H.; Kim, J.; Seung, H.; Yu, W. S.; Koo, J. H.; Yang, J.; Kim, J. H.; Hyeon, T.; Kim, D.-H. Three-Dimensional Foldable Quantum Dot Light-Emitting Diodes. *Nat. Electron.* **2021**, *4* (9), 671–680.
- (12) Shen, H.; Gao, Q.; Zhang, Y.; Lin, Y.; Lin, Q.; Li, Z.; Chen, L.; Zeng, Z.; Li, X.; Jia, Y.; Wang, S.; Du, Z.; Li, L. S.; Zhang, Z. Visible Quantum Dot Light-Emitting Diodes with Simultaneous High Brightness and Efficiency. *Nat. Photonics* **2019**, *13* (3), 192–197.
- (13) Chen, X.; Lin, X.; Zhou, L.; Sun, X.; Li, R.; Chen, M.; Yang, Y.; Hou, W.; Wu, L.; Cao, W.; Zhang, X.; Yan, X.; Chen, S. Blue Light-Emitting Diodes Based on Colloidal Quantum Dots with Reduced Surface-Bulk Coupling. *Nat. Commun.* **2023**, *14* (1), 284.
- (14) Lee, T.; Kim, B. J.; Lee, H.; Hahm, D.; Bae, W. K.; Lim, J.; Kwak, J. Bright and Stable Quantum Dot Light-Emitting Diodes. *Adv. Mater.* **2022**, *34* (4), 2106276.
- (15) Liu, G.; Zhou, X.; Sun, X.; Chen, S. Performance of Inverted Quantum Dot Light-Emitting Diodes Enhanced by Using Phosphorescent Molecules as Exciton Harvesters. *J. Phys. Chem. C* **2016**, *120* (8), 4667–4672.
- (16) Zhang, H.; Sui, N.; Chi, X.; Wang, Y.; Liu, Q.; Zhang, H.; Ji, W. Ultrastable Quantum-Dot Light-Emitting Diodes by Suppression of Leakage Current and Exciton Quenching Processes. *ACS Appl. Mater. Interfaces* **2016**, *8* (45), 31385–31391.
- (17) Ji, W.; Tian, Y.; Zeng, Q.; Qu, S.; Zhang, L.; Jing, P.; Wang, J.; Zhao, J. Efficient Quantum Dot Light-Emitting Diodes by Controlling the Carrier Accumulation and Exciton Formation. *ACS Appl. Mater. Interfaces* **2014**, *6* (16), 14001–14007.
- (18) Ji, W.; Lv, Y.; Jing, P.; Zhang, H.; Wang, J.; Zhang, H.; Zhao, J. Highly Efficient and Low Turn-On Voltage Quantum Dot Light-Emitting Diodes by Using a Stepwise Hole-Transport Layer. *ACS Appl. Mater. Interfaces* **2015**, *7* (29), 15955–15960.
- (19) Wang, F.; Hua, Q.; Lin, Q.; Zhang, F.; Chen, F.; Zhang, H.; Zhu, X.; Xue, X.; Xu, X.; Shen, H.; Zhang, H.; Ji, W. High-Performance Blue Quantum-Dot Light-Emitting Diodes by Alleviating Electron Trapping. *Adv. Opt. Mater.* **2022**, *10* (13), 2200319.
- (20) Park, S. J.; Song, S. H.; Kim, S. S.; Song, J. K. Charge Modulation Layer and Wide-Color Tunability in a QD-LED with Multiemission Layers. *Small* **2021**, *17* (17), 2007397.
- (21) Rhee, S.; Hahm, D.; Seok, H. J.; Chang, J. H.; Jung, D.; Park, M.; Hwang, E.; Lee, D. C.; Park, Y. S.; Kim, H. K.; Bae, W. K. Steering Interface Dipoles for Bright and Efficient All-Inorganic Quantum Dot Based Light-Emitting Diodes. *ACS Nano* **2021**, *15* (12), 20332–20340.
- (22) Wu, Q.; Gong, X.; Zhao, D.; Zhao, Y. B.; Cao, F.; Wang, H.; Wang, S.; Zhang, J.; Quintero-Bermudez, R.; Sargent, E. H.; Yang, X. Efficient Tandem Quantum-Dot LEDs Enabled by An Inorganic Semiconductor-Metal-Dielectric Interconnecting Layer Stack. *Adv. Mater.* **2022**, *34* (4), 2108150.
- (23) Yu, P.; Yuan, Q.; Zhao, J.; Zhang, H.; Ji, W. Electronic and Excitonic Processes in Quantum Dot Light-Emitting Diodes. *J. Phys. Chem. Lett.* **2022**, *13* (13), 2878–2884.
- (24) Zhang, H.; Yuan, Q.; Wang, T.; Xue, X.; Yuan, Y.; Zhang, H.; Zhou, M.; Ji, W. Unraveling the Effect of Shell Thickness on Charge Injection in Blue Quantum-Dot Light-Emitting Diodes. *Appl. Phys. Lett.* **2021**, *119* (24), 243504.
- (25) Wang, T.; Chen, Z.; Zhang, H.; Ji, W. Color-Tunable Alternating-Current Quantum Dot Light-Emitting Devices. *ACS Appl. Mater. Interfaces* **2021**, *13* (38), 45815–45821.
- (26) Kim, J.; Hahm, D.; Bae, W. K.; Lee, H.; Kwak, J. Transient Dynamics of Charges and Excitons in Quantum Dot Light-Emitting Diodes. *Small* **2022**, *18* (29), 2202290.
- (27) Wang, Y.; Zhu, X.; Xue, X.; Chi, X.; Wang, R.; Ji, W. Electron Transport Mechanism in Colloidal SnO₂ Nanoparticle Films and Its Implications for Quantum-Dot Light-Emitting Diodes. *J. Phys. D: Appl. Phys.* **2022**, *55* (37), 374004.
- (28) Sun, Y.; Su, Q.; Zhang, H.; Wang, F.; Zhang, S.; Chen, S. Investigation on Thermally Induced Efficiency Roll-Off: Toward Efficient and Ultrabright Quantum-Dot Light-Emitting Diodes. *ACS Nano* **2019**, *13* (10), 11433–11442.
- (29) Cragg, G. E.; Efros, A. L. Suppression of Auger Processes in Confined Structures. *Nano Lett.* **2010**, *10* (1), 313–317.
- (30) Pal, B. N.; Ghosh, Y.; Brovelli, S.; Laocharoensuk, R.; Klimov, V. I.; Hollingsworth, J. A.; Htoon, H. 'Giant' CdSe/CdS Core/Shell Nanocrystal Quantum Dots as Efficient Electroluminescent Materials: Strong Influence of Shell Thickness on Light-Emitting Diode Performance. *Nano Lett.* **2012**, *12* (1), 331–336.
- (31) Garcia-Santamaria, F.; Chen, Y.; Vela, J.; Schaller, R. D.; Hollingsworth, J. A.; Klimov, V. I. Suppressed Auger Recombination in "Giant" Nanocrystals Boosts Optical Gain Performance. *Nano Lett.* **2009**, *9* (10), 3482–3488.
- (32) Dai, X.; Zhang, Z.; Jin, Y.; Niu, Y.; Cao, H.; Liang, X.; Chen, L.; Wang, J.; Peng, X. Solution-Processed, High-Performance Light-Emitting Diodes based on Quantum Dots. *Nature* **2014**, *515* (7525), 96–99.
- (33) Zhu, B.; Ji, W.; Duan, Z.; Sheng, Y.; Wang, T.; Yuan, Q.; Zhang, H.; Tang, X.; Zhang, H. Low Turn-On Voltage and Highly Bright Ag-In-Zn-S Quantum Dot Light-Emitting Diodes. *J. Mater. Chem. C* **2018**, *6* (17), 4683–4690.
- (34) Yuan, Q.; Guan, X.; Xue, X.; Han, D.; Zhong, H.; Zhang, H.; Zhang, H.; Ji, W. Efficient CuInS₂/ZnS Quantum Dots Light-Emitting Diodes in Deep Red Region Using PEIE Modified ZnO Electron Transport Layer. *Phys. Status Solidi-R* **2019**, *13* (5), 1800575.
- (35) Yu, P.; Zhu, X.; Bai, J.; Zhang, H.; Ji, W. Calibrating the Hole Mobility Measurements Implemented by Transient Electroluminescence Technology. *ACS Appl. Mater. Interfaces* **2022**, *14* (46), 52253–52261.
- (36) Wang, T.; Guan, X.; Zhang, H.; Ji, W. Exploring Electronic and Excitonic Processes toward Efficient Deep-Red CuInS₂/ZnS Quantum-Dot Light-Emitting Diodes. *ACS Appl. Mater. Interfaces* **2019**, *11* (40), 36925–36930.